



Assessments of Heavy Metals Distribution, Contamination and Health Risk in Dagilfani Flood Plains Along River Hadejia



Mikailu Abdullahi.^{1*} & Mohammed Saleh²

¹Department of Physics, Faculty of Natural and Applied Sciences, Sule Lamido University, Kafin Hausa, Jigawa State, Nigeria.

²Department of Physics, Faculty of Physical Science, Bayero University, Kano, Kano State, Nigeria

*Corresponding Author Email: abdulmikailu@gmail.com

ABSTRACT

This study assessed the distribution, contamination status, source characteristics, and health risks of heavy metals in soils from artisanal potash extraction sites within the Dagilfani section of River Hadejia floodplain, Northern Nigeria. The aim of the study is to evaluate heavy metals pollution in an artisan potash extraction site using pollution analysis and to evaluate the impact of heavy metals to public health. Twenty-five topsoil samples were collected and analyzed using Energy Dispersive X-Ray Fluorescence (ED-XRF). Descriptive statistics, Multivariate statistics, pollution Assessment and health risk models were applied for interpretation. The mean concentrations of Al, K, Fe, Mg, Zr, and La exceeded crustal background values, whereas Ca, Ti, Mn, Ce, Zn, and Cr remained below background levels. High coefficients of variation for Ca, Mg, La, Cr, and As indicated strong anthropogenic influence. Correlation analysis (CA), Principal Component Analysis (PCA), and Hierarchical Cluster Analysis (HCA) revealed that Al, K, Fe, Ca, Mg, Ti, Ce, Mn, and Zr were mainly controlled by lithogenic sources. The study also showed that Cr, As, Zn, and La originated from mixed anthropogenic and natural sources linked to agriculture, vehicular emissions, and artisanal activities. Geo-accumulation results showed that the soils were generally unpolluted, although La, Zr, K, and Al exhibited slight to moderate enrichment, with EF values of 2.04 and 1.66 recorded for La and Zr, respectively. Non-carcinogenic risk assessment indicated no significant risk for both adults and children ($HI < 1$). However, carcinogenic risk values for As and Cr ranged from 2.03×10^{-4} to 2.76×10^{-4} , exceeding the USEPA acceptable limit and indicating potential long-term cancer risk.

Keywords:

Carcinogenic,
NonCarcinogenic,
Floodplain,
Contamination,
Potash

INTRODUCTION

Over the past three decades, there has been widespread concern over the link between environmental pollution and human health (Mohammadi et al., 2019). This is particularly the case in locations with a high population density, where the problem of toxic heavy metals in industrial soils has been made worse by industrial modernization and the presence of intensive human activity in urban centers and chemical use in agricultural fields (Krishna & Mohan, 2016). Given its dual roles as a source and sink for metals and other contaminants, the soil is a key indicator of environmental quality (Pobi et al., 2020). Additionally, the nature of the parent rocks as well as the quantity of industrial wastes and fertilizer impurities that reach the soil influence the trace element composition of the soil.

Urban and agricultural soils contaminated with heavy metals have both direct and indirect effects on human health (Oguleye and Akinrinde, 2025; Adimalla, 2019, Wang et al., 2018). The main causes of soil contamination in agricultural and urban areas of the world include industrial development, extensive chemical use in agricultural fields, and municipal waste disposal (Alshahri & El-Taher, 2018; Narsimha, 2018).

The massive increase in heavy metals in urban and agricultural soils may be a contributing factor to soil contamination and a threat to human health. What's even worse is that there is no treatment that can reverse this health impact (Jiang et al., 2017; Chen et al., 2014). Numerous investigations of the contamination of soil with trace elements have been conducted globally and

the effects of these metals on human health were reported (Alshahri & El-Taher, 2018; Adimalla & Wang, 2018). According to Kabata-Pendias, (2010); Ren et al., (2019), high copper consumption impairs the function of the liver, kidneys, and central nervous system. However, according to Jiang et al., (2017) and Wu et al., (2018), lead poisoning can harm the nervous system and result in insomnia, memory loss, and chronic headaches. Ali et al., (2019) and Ren et al., (2019) reported that acute ingestion of Chromium give rise to gastrointestinal disorders and it may sometimes leads to death. Ingestion of cadmium can damage the neurological system and result in renal failure, according to studies by Kabata-Pendias, (2010) and (Yang et al., 2019). Iron (Fe) is another heavy metal of concern. Kabata-Pendias, (2010) reported that Ingestion accounts for most toxic effects of Fe because iron is absorbed rapidly in the gastrointestinal tract. Exposure to high concentrations of Fe exerts adverse effects on target organs, such as liver, the cardiovascular system, and kidneys. According to Zhushan & Shuhua, (2019), prolonged exposure to Arsenic can cause skin cancer, dermal lesions, peripheral neuropathy, and peripheral vascular issues. Soil exposure to heavy metals poses a risk to human health that should not be disregarded. Investigations on the presence of heavy metals in soil centers mostly on areas that are highly developed, such as industrial areas and urban accumulations, as well as areas that include linear and constant emitters, such as industrial facilities, landfills, and roads (Krishna & Mohan, 2016). Numerous studies have shown that industrial districts' soils are contaminated with heavy metals (Hussain et al., 2018; Gorostiza & Sauri, 2019; Ilechukwu et al., 2021). Numerous numerical approaches have been utilized in literature to assess the quality of soil. Choosing a reliable and appropriate approach to evaluate soil quality and gain a thorough understanding of soil contamination is therefore crucial for decision-making and spatial planning.

Pollution indices are effective instruments for processing, analyzing, and disseminating unprocessed environmental

data to managers, decision-makers, health professionals, and the general public Soltani-gerdefaramarzi et al., 2021; Adimalla, 2019). In this study, pollution indices were used to assess the soil of the study area. The indices used were Geo-accumulation Index (GI), Pollution Load Index (PLI) and Contamination Factor (CF). In addition, Carcinogenic and non-carcinogenic impacts of heavy metals on human health were evaluated using Chronic Daily Dose (CDD), Hazard Quotient (HQ) and Hazard Index (HI). Therefore, the purpose of this study is to evaluate heavy metals pollution in an artisan potash extraction site using pollution analysis and to evaluate the impact of heavy metals to public health.

Dagilfani is an agrarian community along the flood plains of River Hadejia. The people living in the area partake in all year-round farming activities, fishing and artisan potash extraction. However, in the research area, no assessments of the health risks associated with heavy metal pollution in soils have been conducted. This indicates a knowledge gap about the potential adverse effects of soil heavy metals on human health. As a result, the objective of this research is to (i) analyze the distribution of heavy metals in the study area, and then use multivariate statistics to determine their source. (ii) Use the geo accumulation index, enrichment factor, and contamination factor, to calculate the extent of soil pollution; (iii) to determine the potential effects of soil heavy metal exposure on both adult and child health through various pathways. The study will close a gap in the literature by describing the health impacts caused by the presence of heavy metals in the study area.

THE STUDY AREA

The study area is a town in Birniwa Local Government Area of Jigawa State. It is located within latitude 12.72 and 12.82 and longitude 10.30 to 1038. The topography of the area is a flat terrain and its geology is of Consolidated Sedimentary Chad Formation. The consolidated sediments consist of mostly silt, sand and clay shale and their feldspath (Orisakwe, 2013).

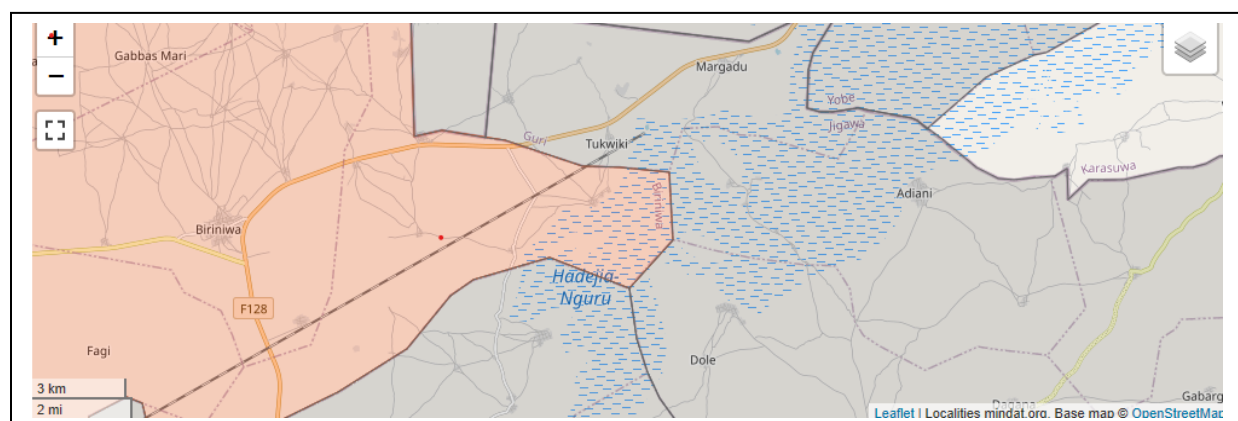


Fig 1: A Map showing the study area

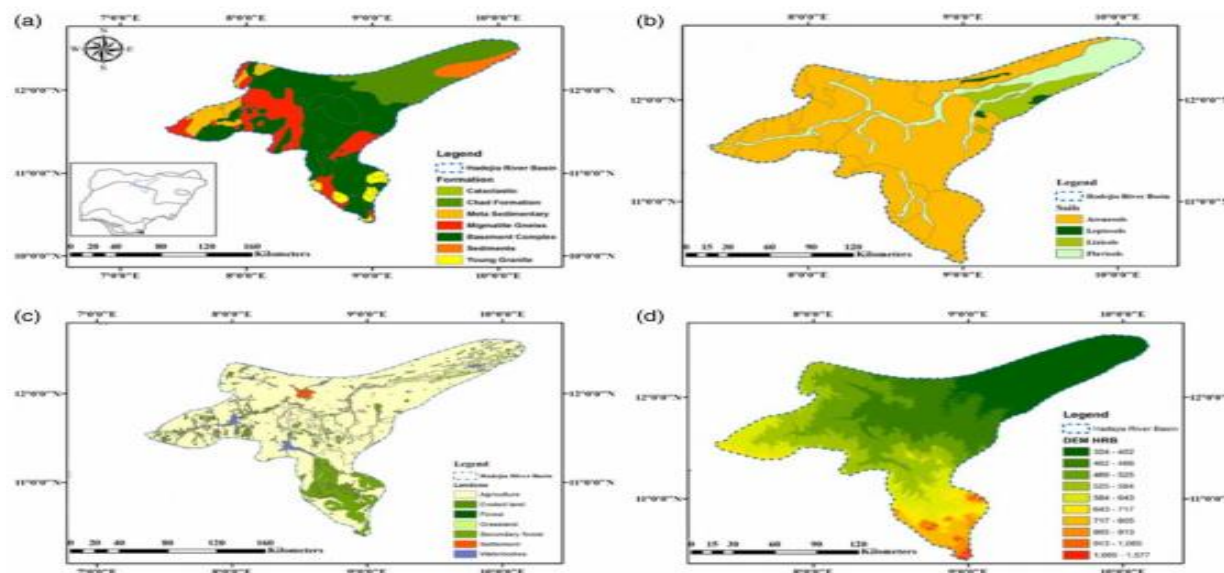


Fig 2: Map showing (a) the geology, (b) the soils, (c) the major land use and (d) spatial variation in elevation within Hadejia River Basin. (Source: Umar et al., 2019)

The area is located in an inland drainage system of Lake Chad basin and River Hadejia flows through it. It is in the tropical region with wet season lasting from June through September and the dry season beginning in October and lasting until May (Orisakwe, 2013). The temperature of the area varies from 12°C between December and January and 40°C recorded between March and April (Dauda et al., 2017).

MATERIALS AND METHODS

The following Materials and methods were used in this work:

Sample collection and preparation: The following materials were used for sample collection and preparation: plastic hand trowel, self-locking polythene bags, handheld Global positioning System (GPS) device and plastic containers for sample storage.

Twenty-five samples were collected from the upper 15cm of the soil and each sample was a composite of three subsamples from nearby sites (approximately 3m apart). The samples were collected with stainless steel shovel and Global Positioning System (GPS) was used to record the coordinates of the sampling points. The samples were air dried at room temperature in the laboratory and impurities such as stones and plant roots were removed. The samples were then sieved through a mesh.

XRF Analysis: The samples collected in this study were analyzed using Energy Dispersive X-Ray Fluorescence. In recent times, trace element concentration is being measured using X-Ray Fluorescence Technique which operates well and successfully offers a quick, affordable and substantially accurate results (Wang et al., 2020;

Oyedotun, 2018; Shackley, 2018). In this study the concentrations of the trace elements were analyzed using ED-XRF at the Centre for Dry Land Agriculture (CDA), Bayero University, Kano. The instrument (Bruker S2 Ranger) was fitted with a side window X-Ray Tube (50W) that has a silver anode. It has a Silicon Drift Detector with high sensitivity and resolution.

Statistical Analysis: In order to determine the distribution and correlation of the variables under consideration, statistical methods were used to examine the analytical data acquired. In this work Descriptive and Multivariate statistical were considered. The parameters used were:

Descriptive Statistical Analysis: The following descriptive tools were used: Mean, Standard Deviation, Minimum and Maximum, Skewness and Kurtosis. The standard deviation was calculated to show the degree of discrete distribution of various metal concentrations and to infer indirectly the activity of the selected metal in the research area. Different distribution of metals is revealed through the application of Skewness. In this study Microsoft Excel from Microsoft Corporation and Origin Pro 8.5 from OriginLab Corporation.

Principal Component Analysis (PCA): Principal component analysis (PCA) is a technique that was used to help with the understanding of source data (Jin et al., 2019). This effective technique enables the identification of several metal groups that correlate and may therefore be thought of as sharing a common origin and comparable behavior (Chandrasekaran et al., 2015; Qishlaqi & Moore, 2007), In order to achieve equal contribution,

each variable in this study is normalized to a unit variance and PCA is applied to the correlation matrix. This is as a result of the varying orders of magnitude in the concentration of the metals assessed in this study. To maximize the variance of the factor loadings across variables for each factor, PCA with varimax normalized rotation is utilized to get an easily interpretable output. Factor loadings of 0.32 are often rated as extremely poor and 0.7 as outstanding (Chandrasekaran & Ravisankar, 2015).

Cluster Analysis: In research literature CA was the second-most popular multivariate statistical analysis technique (45%) (Hou et al., 2017). CA allows for the grouping of a collection of data objects into groups based on shared traits. Numerous CA techniques are available that maximize inter-group variability while minimizing intragroup variability (Zhang et al., 2018). According to (Hou et al., 2017), CA has frequently been employed to verify PCA results for investigations of the distribution of regional soil heavy metals.

Pearson Correlation Analysis: Pearson correlation analysis is one of the most widely used statistical tool in the reviewed studies (Hou et al., 2017; Krishna & Mohan, 2016). The results of this analysis are expressed as a correlation coefficient, which can range from 0 to 1, with 1 denoting a perfect positive linear relationship, 0 indicating no correlation and -1 denoting a perfect negative linear relationship (Hou et al., 2017).

Quantification of soil pollution:

The goal of quantifying soil pollution is to determine the extent of the contamination as well as any potential anthropogenic effects on the soil. The enrichment factor (EF), geo-accumulation index (I_{geo}), contamination factor (CF), and pollution load index (PLI) for the metals found in soil samples taken from the study area were calculated.

Enrichment Factor (EF): EF is the most crucial method used in determining how heavily contaminated an area is with heavy metals (Adimalla et al., 2020; Wu et al., 2018). Each heavy metal's EF value in the soil is calculated using

$$EF = \frac{(C_n)_{sample}}{(C_{ref})_{sample}} / \frac{(B_n)_{background}}{(B_{ref})_{background}} \quad (1)$$

where $(C_n)_{sample}$ is the concentration of the examined element, $(C_{ref})_{sample}$ is the concentration of the reference element in the examined environment, $(B_n)_{background}$ is the crustal value of the examined element and $(B_{ref})_{background}$ is the crustal value of the reference element. A metal with an EF value between 0 and 1.5 may have come entirely from crustal materials or from natural weathering processes, but a metal with an EF value greater than 1.5 is said to have come from

anthropogenic activity (Chandrasekaran et al., 2015). Typically, EF consists of five grades, namely deficiency ($EF \leq 1.5$), minor ($1.5 < EF \leq 3.0$), moderate ($3.0 < EF \leq 5.0$), severe ($5.0 < EF \leq 10$), and very severe anthropogenic influence ($EF > 10$) (Adimalla et al., 2020; Adimalla & Wang, 2018; Ni et al., 2018).

Geo-accumulation Index (GI): The geo-accumulation index, developed by Muller (1969) to reflect the level of anthropogenic heavy metal enrichment in local soil or sediment, is commonly employed in the assessment of heavy metal contamination (Zheng et al., 2020). In this study, the geo-accumulation index for heavy metals was determined using the equation

$$I_{geo} = \log_2 \left(\frac{C_n}{k B_n} \right) \quad (2)$$

C_n is heavy metal concentration in soil sample and $k B_n$ is average geochemical background value of the measured heavy metal. Muller classified seven levels of the GI namely, not polluted, $GI < 0$; not polluted to moderately polluted, $0 < GI \leq 1$; moderately polluted, $1 < GI \leq 2$; moderately polluted to heavily polluted, $2 < GI \leq 3$; heavily polluted, $3 < GI \leq 4$; heavily polluted to extremely polluted, $4 < GI \leq 5$; and extremely polluted, $GI > 5$.

Human Health Risk Assessment:

A health risk assessment is used to distinguish between risks that exposure to chemicals poses for human health. that are carcinogenic and non-carcinogenic (Doabi et al., 2018; Hu et al., 2019; Kouchou et al., 2020; Narsimha, et al., 2019; Wang et al., 2020; Obiri-nyarko et al., 2021; . It is typically used to calculate the risks of both carcinogenic and non-carcinogenic risks via inhalation, dermal and dietary exposure pathways (Adimalla & Wang, 2018). The technique employed in this study is based on recommendations from the United States of America Environmental Protection Agency (USEPA) exposure factors handbook (USEPA, 1986).

Non-carcinogenic Risk Assessment: In accordance with USEPA Protocol 1989 and 2004 Equations 5, 6, and 7 can be used to calculate the dose for a non-carcinogenic effect. The equations are as follows:

$$CDD_{ing} = \frac{C \times ingR \times EF \times ED}{BW \times AT} \times CF \quad (5)$$

$$CDD_{inh} = \frac{C \times inhR \times EF \times ED}{PEF \times BW \times AT} \quad (6)$$

$$CDD_{dermal} = \frac{C \times SAF \times SA \times DAF \times EF \times ED}{BW \times AT} \times CF \quad (7)$$

Where CDD_{ing} , CDD_{inh} and CDD_{dermal} are the daily dose via hand to mouth ingestion of soil substrate particles, daily dose via inhalation of suspended particles through mouse and nose and daily dose via dermal absorption of elements adhered to exposed skin respectively. The meanings and values of the other parameters used in equations 5, 6 and 7 were given in Table 1.

Table 1: Parameters used in calculating daily dose of heavy metals in Adults and Children

Parameter/Unit	Meaning	Adult	Children	Reference
C (mg/Kg)	Concentration of metal in the soil			This study
ingR (mg/day)	Ingestion Rate of Soil	100	200	USEPA (1989)
EF (days/year)	Exposure Frequency	350	350	USEPA (2002)
ED (years)	Exposure Duration	24	6	USEPA (2002)
CF (Kg/mg)	Conversion Factor	1×10^{-6}	1×10^{-6}	USEPA (2002, 1989)
AT (years)	Average Time	8760	2190	USEPA (2002)
BW (Kg)	Body Weight of the Exposed Individual	55.9	15	Adimalla, (2019), Aluko (2018)
inhR (m ³ /day)	Inhalation Rate of Soil	20	5	USEPA (2002)
PEF (m ³ /Kg)	Particle Emission Factor	1.36×10^9	1.36×10^9	USEPA (2002)
SAF (mg/cm ²)	Skin Adherence Factor	0.7	0.2	USEPA (2002)
SA (cm ²)	Exposed Skin surface Area	4350	1600	USEPA (2002)
DAF	Dermal Absorption Factor	0.001	0.001	USEPA (2002)

Non-carcinogenic hazards are characterised by Hazard Quotient (HQ). HQ is a unitless number that represents the likelihood that a person will have adverse effects. (Aluko et al., 2018). It is defined as the quotient of the chronic daily intake or the dose divided by toxicity threshold value which is referred to as the Reference Dose (RfD) for a specific substance (Adimalla, 2019). Wu et al., (2018) reported that HQ is determined using equation 8.

$$HQ = \frac{CDD}{RfD} \quad (8)$$

Where CDD is the Acceptable Daily Intake. To determine the overall potential for non-carcinogenic effect posed by more than one substance, the total exposure Hazard Index (HI) is utilized. The HI is computed as the sum of all HQs i.e.

$$HI = \sum HQ = \sum \frac{CDD}{RfD} \quad (9)$$

There is no risk of a non-carcinogenic effect if the determined value of HI is less than 1, but if it is larger than 1, it implies a possibility of such an impact on humans (USEPA, 1989). The values of RfD were given in Table 2.

Table 2: Reference Doses and Slope Factors of Heavy Metals

Metals	Reference Dose			Slope Factor	Reference
	Ingestion	Inhalation	Dermal		
Cr	3×10^{-3}	2.86×10^{-5}	6×10^{-5}	0.50 (ingestion) 0.42 (inhalation) 0.20 (Dermal)	(USEPA, 2010; USEPA, 2012)
Mn	4.6×10^{-2}	1.433×10^{-5}	1.84×10^{-3}		(USEPA, 2010)
Zn	3×10^{-1}	3×10^{-1}	6×10^{-2}		(USEPA, 2010)
As	3×10^{-4}	1.23×10^{-4}	1.23×10^{-4}	1.50 (ingestion) 15 (inhalation) 1.5 (Dermal)	(USEPA, 2010; USEPA, 2012)
Fe	7×10^{-1}	8×10^{-1}	7×10^{-1}		(USEPA, 2010)

Carcinogenic Risk Assessment: The Carcinogenic Risk Assessment is used to calculate the lifetime risk of developing cancer as a result of exposure to suspected carcinogens. (Yaw et al., 2019, Adimalla, 2019). According to USEPA (1989), equation 11 is used to compute the lifetime carcinogenic risk (CR) for a person, and equation 12 is used to calculate the total carcinogenic risk (TCR), which is the sum of the risks from all exposure paths for each individual metal.

$$CR = CDD \times SF \quad (11)$$

$$TCR = \sum CR \quad (12)$$

Where CDD is the Chronic Daily Dose and SF is the Slope Factor and its values were listed in Table 2. According to USEPA (2001), the range of acceptable TCR for regulatory purposes is 1×10^{-6} to 1×10^{-4} , therefore $TCR \leq 1 \times 10^{-6}$ represents virtual safety while $TCR \geq 1 \times 10^{-4}$ indicates potential risk.

RESULTS AND DISCUSSION

Descriptive Statistics: Descriptive data analysis comprising mean, minimum, maximum, standard

deviation, Skewness, kurtosis and coefficient of variation (CV) were carried out and the results were presented in Table 2: Descriptive Statistics of Elements in Dagilfani Table 1.

S/N	Elem	No. of Obser	Mean	Min.	Max.	Stand. Dev.	Skew.	Kurt.	CV (%)	*Crustal Values
1	Al	25	41569	23800	56600	7987.47	-0.22	0.54	19.22	25000
2	K	25	20750	10600	37600	6457.76	1.11	1.96	31.12	10700
3	Fe	25	15106	6100	24600	5991	0.42	-1.08	39.66	9800
4	Ca	25	7850	3500	52200	4686	1.40	0.99	59.69	39100
5	Ti	25	847	500	1090	152.7	-0.47	0.24	18.03	1500
6	Mg	25	7615	0	14000	4215	0.10	-0.37	68.11	7000
7	Zr	25	495	340	610	88.09	-0.34	-1.21	17.80	220
8	Mn	25	625	0	700	280.4	1.30	-0.31	44.86	850
9	La	25	96.15	0	120	40.7	-1.37	0.64	52.09	30
10	Ce	25	70.71	0	100	27.38	-1.40	2.04	44.25	92
11	Zn	25	14.44	0	50	19.96	0.70	-1.52	14.45	16
12	Cr	25	31.67	0	35	15.9	0.60	-1.84	50.22	35
13	As	25	13.4	0	25	8.29	1.69	1.62	56.13	13.0

* The Crustal value reported by Turekian and Wedephol, (1961); n = 25

The mean concentration of Al, K, Fe, Ca, Mg, Ti, Zr, La, Ce, Mn, Cr, As and Zn were found to be 41569, 20750, 15106, 7850, 7615, 847, 495, 96.15, 70.71, 625, 31.67, 18 and 39.17 respectively. The concentrations of Al, K, Fe, Mg, Zr and La are greater than the crustal value reported by Turekian and Wedephol, (1961) while concentrations of Ca, Ti, Mn, Ce, Zn and Cr are less than the crustal values. The earth's crust background values reported by Turekian and Wedephol, (1961) were used, despite the advantages and disadvantages of its use (Abraham & Parker, 2008; Pablo et al., 2016). This is due to lack of local reference values for metal concentration.

Based on the analysis using Variation Coefficients (CV), Ca, Mg, La, Cr and As shows wider variability ($CV \geq 50$). This variability indicates high interference of anthropogenic activities as reported by Gupta et al.,

(2021) and Jiang et al., (2019). The CV for Al, K, Fe, Ti, Zr, Mn, Ce, and Zn was less than 50%, indicating moderate variability and pointing to relatively uniform spatial variation of these metals with little changes as reported by Wang et al., (2020). The coefficient of variation (CV) was calculated in order to evaluate the spatial variation of trace metal concentrations within the study region as well as to indirectly demonstrate the degree of dispersed distribution of metal concentrations (Gupta et al., 2021). The Skewness and kurtosis of K, As and Ce are, however, considerably bigger than those of the other heavy metals, indicating that certain soil samples are from high concentration locations with high rates of accumulation as reported by Zhang et al., (2018).

Correlation Analysis: The origin and migration of trace metals may be revealed via correlations between the metals (Hu et al., 2019). The findings of the Pearson correlation study are presented in Table 2.

Table 3: Correlation coefficients Matrix of trace metals in the study area

	Al	K	Fe	Ca	Mg	Ti	Zr	La	Ce	Mn	Cr	As	Zn
Al	1.000												
K	0.661	1.000											
Fe	0.920	0.804	1.000										
Ca	0.712	0.552	0.725	1.000									
Mg	0.798	0.511	0.790	0.529	1.000								
Ti	0.514	0.793	0.711	0.496	0.529	1.000							
Zr	0.258	0.099	0.324	0.259	0.247	0.553	1.000						

La	0.016	0.001	-0.120	0.176	-0.270	-0.453	-0.483	1.000					
Ce	0.811	0.380	0.711	0.571	0.598	0.150	0.093	0.285	1.000				
Mn	0.529	0.314	0.668	0.688	0.667	0.517	0.463	-0.311	0.506	1.000			
Cr	0.009	0.073	-0.095	-0.144	-0.234	-0.364	-0.585	0.408	0.137	-0.444	1.000		
As	0.137	-0.310	-0.105	-0.088	0.060	-0.412	-0.044	0.171	0.186	-0.141	-0.076	1.000	
Zn	0.077	-0.245	-0.004	0.278	0.042	0.066	0.385	-0.137	-0.045	0.245	-0.480	0.034	1.000

From Table 2, the heavy metals Cr, As and Zn were not significantly correlated with any other metal. However, there is very significant correlation ($p < 0.001$) were found between Al – K (0.661), Al – Fe (0.920), Al – Ca (0.712), Al – Mg (0.798), Al – Ce (0.811), K – Fe (0.804), K – Ti (0.793), Fe – Ca (0.725), Fe – Ti (0.711), Fe – Ce (0.711), Fe – Mn (0.668), Ca – Mn (0.688) and the result also showed a significant correlation ($p < 0.05$) between Ti – Zr (0.553). This result revealed that Al, K, Fe, Ca, Mg, Ce, Ti, Mn and Zr might originate from a common source.

The result also revealed that the distribution of Cr, As, Zn and La were also controlled by a common source. This is in agreement with the findings of Yaw *et al.*, (2019); Pujiwati *et al.*, (2018).

Principal Component Analysis (PCA): In this work, PCA was computed using SPSS Statistical package. It is used in order to compute the factor loadings that involved in the contribution of metal concentration and source apportionment.

Table 4: Total Variance Explained for the PCA, component matrices and rotated component matrices

Component	Initial Eigenvalues			Extraction Sums of Squared Loadings			Rotation Sums of Squared Loadings		
	Total	% of Variance	Cumulative %	Total	% of Variance	Cumulative %	Total	% of Variance	Cumulative %
1	5.605	43.114	43.114	5.605	43.114	43.114	5.073	39.023	39.023
2	2.524	19.418	62.532	2.524	19.418	62.532	2.229	17.146	56.169
3	1.673	12.871	75.403	1.673	12.871	75.403	1.815	13.965	70.134
4	1.013	7.791	83.194	1.013	7.791	83.194	1.698	13.060	83.194
5	.639	4.918	88.113						
6	.493	3.795	91.908						
7	.480	3.693	95.601						
8	.279	2.143	97.744						
9	.148	1.136	98.881						
10	.072	.555	99.435						
11	.051	.391	99.826						
12	.015	.112	99.938						
13	.008	.062	100.000						

Extraction Method: Principal Component Analysis.

Component Matrix ^a					Rotated Component Matrix ^a				
	Component					Component			
	1	2	3	4	1	2	3	4	
Al	.881	.331	.176	-.107	.963	.019	.013	-.033	
K	.729	.295	-.504	.043	.693	.057	-.273	.562	
Fe	.956	.201	-.076	-.062	.942	.162	-.011	.225	
Ca	.793	.155	.180	.439	.770	-.186	.429	.259	
Mg	.831	.062	.107	-.322	.829	.343	-.019	-.076	
Ti	.777	-.301	-.477	.015	.528	.527	.059	.602	
Zr	.480	-.658	.104	-.044	.221	.627	.478	.076	
La	-.214	.710	.274	.469	.061	-.913	.009	-.093	
Ce	.663	.514	.364	-.047	.852	-.250	.011	-.221	
Mn	.791	-.241	.167	.068	.656	.324	.410	.112	
Cr	-.285	.771	-.259	.013	-.023	-.609	-.606	.063	
As	-.123	.165	.740	-.485	.104	-.031	-.008	-.902	
Zn	.153	-.537	.500	.484	-.022	.065	.888	-.044	

Extraction Method: Principal Component Analysis.
a. 4 components extracted.

Extraction Method: Principal Component Analysis.
Rotation Method: Varimax with Kaiser Normalization.
a. Rotation converged in 6 iterations.

In this study the components were extracted using Varimax Rotation Method. The results of the PCA were presented in Table 3. The results obtained show that the first four principal components (PC1 to PC4) have an Eigen value greater than 1 and comprised 83.194 % of the cumulative variance. PC1 explains 43.114% of the total variance with significant positive loadings of Al, K, Fe, Ca, Mg, Ti, Ce, Mn and Zr. It would be more accurate to describe these metals as being derived from natural sources, implying that they are derived from parent rocks. PC2 accounted for 19.418% of total variance with significant positive loading of La (0.710), and Cr (0.771). PC3 accounted for 12.87% of the total variance and have high loadings of As (0.740) and Zn (0.500). These two last components represent the mixed sources of elements, which include atmospheric deposition, agricultural activities, automobile emissions, and natural activities. It can be inferred from the results of PCA that natural and anthropogenic activities both contributed to the existing concentration of metals in the soil of the study area. The anthropogenic activities include emissions of vehicles, which is confirmed from the fact that soil samples were taken along the major highway connecting a number of villages that have habitation. The result is in agreement with the findings of Chandrasekaran, et al., 2015. The result of the PCA is also in agreement with those of the Correlation Analysis which showed that Al, K, Fe, Ca,

Mg, Ce, Ti, Mn and Zr might originate from a common source and also revealed that the distribution of Cr, As, Zn and La were also controlled by a common source.

Hierarchical Cluster Analysis (HCA): The essence of HCA in this study is to find out the origin of metals, similarity in distribution and their behavior during their stall in the soil. The result of the HCA is depicted using a dendrogram (Fig 2). The dendrogram produced by the HCA on the parameters evaluated can be divided into four major clusters using Ward's technique and the squared Euclidean distance as a similarity measure. The results of the cluster analysis revealed that cluster 1 can be used to classify all the heavy metals under study. Elements found in Cluster 1 include As, Zn, Cr and La. These pollutants were derived from mixed sources of anthropogenic and natural sources. The metals present in cluster 2 were Ce and Mn while those in cluster 3 were Zr, Ca, Ti and Mg. The metals in cluster 4 includes K, Fe and Al. The metals in Clusters 2, 3 and 4 were from parent rock materials and are mainly generated from natural sources such as surface run offs and presence of some metal bearing minerals (Chandrasekaran et al., 2015). The result is in agreement with both PCA and CA analysis. It is also in agreement with the findings of Abowaly *et al.*, (2021), who, in their study of the Nile Delta, identified a strong geogenic association among elements commonly found in evaporitic settings.

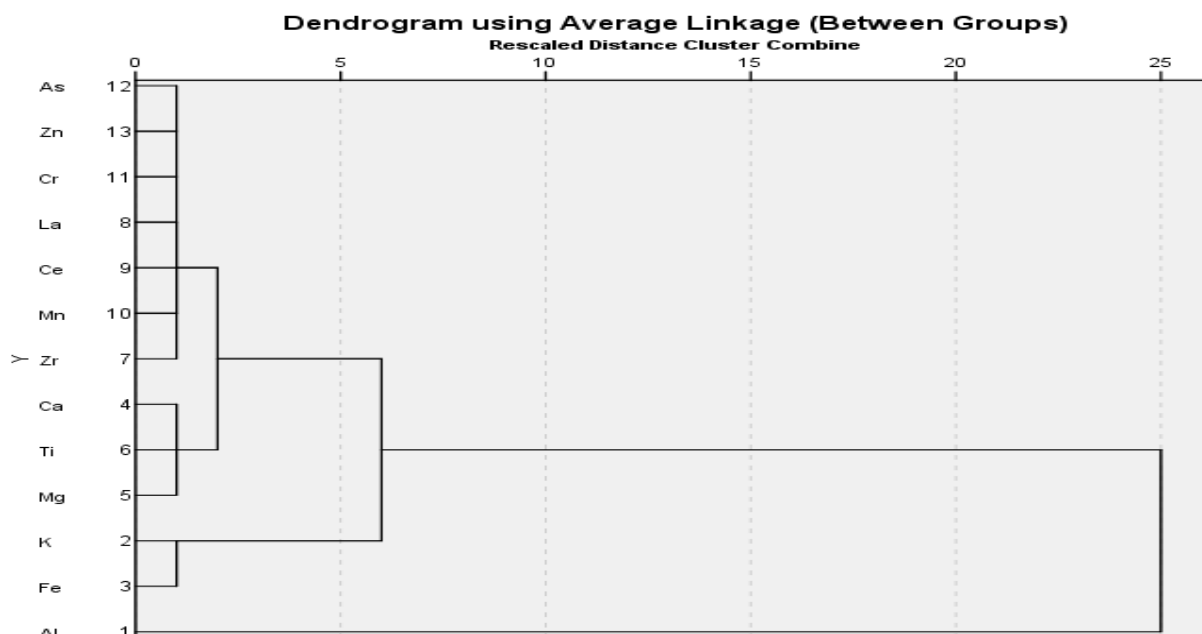


Fig. 2: The Dendrogram depicting the Hierarchical Clustering of Metals

Geo-Accumulation Index: The index of geo-accumulation is extensively used worldwide to determine the degree of metal pollution (Adimalla & Wang, 2018; Mamat et al., 2018). The results of the GI values were shown in Table 4. From the Table it can be seen that the mean GI values of the metals decreased in the order, Ca (-3.09) < Ti (-1.89) < Ce (-0.87) < Mg (-0.48) < Zn (-0.39) < Cr (-0.27) < Mn (-0.25) < As (-0.20) < Fe (-0.07) < Al (0.12) < K (0.31) < Zr (0.56) < La (0.88). Overall, the mean value of Geo-accumulation index for all the metals, obviously indicates that soil of the study

region was not polluted by Ca, Ti, Ce, Mg, Zn, Cr, Mn, As and Fe. The result also showed that the study area is not polluted to moderately polluted by Al, K, Zr and La. Generally, La had the highest index of GI ranging from 0.83 to 1.40, in which about 62.5% of soil sampling sites were not polluted to moderately polluted, whereas 37.5 of the sampling sites falls in moderately polluted. It can be deduced from the result that the sampling site is not polluted by the heavy metals Zn, Cr, Mn and As. This is in agreement with the findings of Chandrasekaran et al., (2015).

Table 5: The Values for Geo Accumulation Index and Contamination Factor for the study area.

S/No	Metal	Mean Concentration	Background Value	Geo accumulation Index			Enrichment Factor
				Min	Max	Mean	
1	Al	41569	25000	-0.6559	0.5939	0.1214	1.17
2	K	20750	10700	-0.0880	1.2282	0.3091	1.35
3	Fe	15106	9800	-1.2689	0.7428	-0.0719	-
4	Ca	7850	39100	-4.0667	-1.6646	-3.0995	0.13
5	Mg	6188	7000	-0.3923	0.4150	-0.4769	0.53
6	Ti	846.9	1500	-1.2902	-1.4339	-1.4339	0.41
7	Zr	495	220	0.0431	0.8863	0.5621	1.66
8	La	78.13	30	0.8301	1.4150	2.2222	2.04
9	Ce	61.88	19	-1.4647	-0.4647	-0.8657	0.44
10	Mn	625	850	-1.0875	-0.8651	-0.2579	0.84
11	Cr	31.67	35	-0.8074	-0.5850	-0.2749	0.26
12	As	13.4	13	-0.9634	-0.3785	-0.2043	0.27
13	Zn	14.44	16	-1.2630	-0.2630	-0.3979	0.39

Enrichment Factor: Enrichment Factor can be used to gauge the extent of anthropogenic influence on soil

contamination by various metals and as it can provide tools to differentiate an anthropogenic source from a

natural process. The enrichment factor values were given in Table 4. The Enrichment Factor values obtained from the concentration of metals in the study area showed that all the metals in the study area fall within the range 0 to 1.5 except Zr (1.66) and La (2.04) whose values were greater than 1.5. This implies that all the metals except Zr and La may have come entirely from crustal materials or from natural weathering processes while Zr and La may have come from mixed sources of natural processes and anthropogenic activity (Chandrasekaran et al., 2015). The result also showed that the EF values of the studied metals are within $1.5 < EF \leq 3.0$ which according to Adimalla & Wang, 2018 and Ni et al., 2018 indicates deficiency in minimum enrichment. This result is in conformity with the findings of Chandrasekaran & Ravisankar, (2015).

Human Health Risk Assessment: Table 8 displays the findings on the non-carcinogenic and carcinogenic health risks of five metals related to exposure in soils by ingestion, inhalation, and dermal contacts. Ackah, 2019; Long et al., 2021; Penteado et al., 2021; Thongyuan et al., 2021 reported that there is no risk of a non-carcinogenic effect if HI is less than 1, but that there is a possibility of a non-carcinogenic effect on humans if HI is larger than 1. In the case of carcinogenic risk, the permitted TCR range for regulatory reasons is 1×10^{-6} to 1×10^{-4} , therefore $TCR \leq 1 \times 10^{-6}$ represents virtual safety while $TCR \geq 1 \times 10^{-4}$ suggests potential risk.

Table 8: Results of non-carcinogenic risks for children in the study area

			Fe	Mn	Cr	As	Zn
Ingestion	CDD	Min	7.79×10^{-2}	0	0	0	0
		Max	3.15×10^{-1}	8.95×10^{-3}	4.47×10^{-4}	1.92×10^{-4}	2.56×10^{-4}
		Mean	1.93×10^{-1}	7.99×10^{-3}	4.05×10^{-4}	1.37×10^{-4}	1.85×10^{-4}
	HQ	Min	1.11×10^{-1}	0	0	0	0
		Max	4.49×10^{-1}	1.95×10^{-1}	1.49×10^{-1}	6.39×10^{-1}	8.52×10^{-3}
		Mean	2.76×10^{-1}	1.74×10^{-1}	1.35×10^{-1}	4.56×10^{-1}	6.16×10^{-3}
Inhalation	CDD	Min	1.48×10^{-6}	0	0	0	0
		Max	5.96×10^{-6}	1.69×10^{-7}	8.48×10^{-9}	3.63×10^{-9}	4.84×10^{-9}
		Mean	3.66×10^{-6}	1.51×10^{-7}	7.67×10^{-9}	2.59×10^{-9}	3.49×10^{-9}
	HQ	Min	1.85×10^{-6}	0	0	0	0
		Max	7.44×10^{-6}	1.18×10^{-2}	2.96×10^{-4}	2.95×10^{-5}	1.61×10^{-8}
		Mean	4.57×10^{-6}	1.06×10^{-2}	2.68×10^{-4}	2.11×10^{-5}	1.17×10^{-8}
Dermal	CDD	Min	1.25×10^{-4}	0	0	0	0
		Max	5.03×10^{-4}	1.43×10^{-5}	7.16×10^{-7}	3.07×10^{-7}	4.09×10^{-7}
		Mean	3.09×10^{-4}	1.28×10^{-6}	6.48×10^{-7}	2.19×10^{-7}	2.95×10^{-7}
	HQ	Min	1.78×10^{-4}	0	0	0	0
		Max	7.19×10^{-4}	7.78×10^{-3}	1.19×10^{-2}	2.49×10^{-3}	6.82×10^{-6}
		Mean	4.41×10^{-4}	6.95×10^{-3}	1.08×10^{-2}	1.78×10^{-3}	4.92×10^{-6}
HI	Min	1.12×10^{-1}	0	0	0	0	
	Max	4.50×10^{-1}	2.14×10^{-1}	1.61×10^{-1}	6.42×10^{-1}	8.53×10^{-3}	
	Mean	2.76×10^{-1}	1.91×10^{-1}	1.46×10^{-1}	4.58×10^{-1}	6.16×10^{-3}	

Table 9: Results of non-carcinogenic risks for adults in the study area

			Fe	Mn	Cr	As	Zn
Ingestion	CDD	Min	1.04×10^{-1}	0	0	0	0
		Max	4.22×10^{-1}	1.20×10^{-2}	6.00×10^{-4}	2.57×10^{-4}	3.43×10^{-4}
		Mean	2.59×10^{-1}	1.07×10^{-2}	5.43×10^{-4}	1.84×10^{-4}	2.48×10^{-4}
	HQ	Min	1.49×10^{-1}	0	0	0	0
		Max	6.03×10^{-1}	3.73×10^{-1}	2.00×10^{-1}	8.58×10^{-1}	1.14×10^{-2}
		Mean	3.70×10^{-1}	1.42×10^{-1}	1.81×10^{-1}	6.12×10^{-1}	8.26×10^{-3}
Inhalation	CDD	Min	1.59×10^{-6}	0	0	0	0
		Max	6.39×10^{-6}	1.82×10^{-7}	9.09×10^{-9}	3.89×10^{-9}	5.19×10^{-9}
		Mean	3.93×10^{-6}	1.62×10^{-7}	8.23×10^{-9}	2.78×10^{-9}	3.75×10^{-9}
	HQ	Min	3.94×10^{-5}	0	0	0	0
		Max	1.59×10^{-4}	5.87×10^{-4}	3.18×10^{-4}	3.17×10^{-5}	1.73×10^{-8}

		Mean	9.77×10^{-5}	5.24×10^{-4}	2.88×10^{-4}	2.26×10^{-5}	1.25×10^{-8}
Dermal	CDD	Min	3.19×10^{-5}	0	0	0	0
		Max	1.28×10^{-4}	3.66×10^{-6}	1.83×10^{-7}	7.84×10^{-8}	1.04×10^{-7}
		Mean	7.89×10^{-5}	3.26×10^{-6}	1.65×10^{-7}	5.59×10^{-8}	7.54×10^{-8}
	HQ	Min	4.55×10^{-5}	0	0	0	0
		Max	1.84×10^{-4}	1.99×10^{-3}	3.05×10^{-3}	6.37×10^{-4}	1.74×10^{-6}
		Mean	1.13×10^{-4}	1.77×10^{-3}	2.76×10^{-3}	4.54×10^{-4}	1.26×10^{-6}
HI	Min	1.49×10^{-1}	0	0	0	0	
	Max	6.03×10^{-1}	2.64×10^{-1}	2.03×10^{-1}	8.58×10^{-1}	1.14×10^{-2}	
	Mean	3.70×10^{-1}	2.35×10^{-1}	1.84×10^{-1}	6.12×10^{-1}	8.26×10^{-3}	

Table 10: Carcinogenic risks for adults and children in the study area

Path		Carcinogenic Risk (Arsenic)		Carcinogenic Risk (Chromium)	
		Children	Adults	Children	Adults
Ingestion	Min	0	0	0	0
	Max	2.88×10^{-4}	3.86×10^{-4}	2.23×10^{-4}	3.00×10^{-4}
	Mean	1.37×10^{-4}	2.76×10^{-4}	2.03×10^{-4}	2.72×10^{-4}
Inhalation	Min	0	0	0	0
	Max	5.45×10^{-8}	5.85×10^{-8}	3.48×10^{-7}	3.73×10^{-7}
	Mean	3.89×10^{-8}	4.17×10^{-8}	3.14×10^{-7}	3.37×10^{-7}
Dermal	Min	0	0	-	-
	Max	4.61×10^{-7}	1.18×10^{-7}	-	-
	Mean	3.29×10^{-7}	8.39×10^{-8}	-	-
Total Cancer Risk	Min	0	0	0	0
	Max	2.88×10^{-4}	3.86×10^{-4}	2.24×10^{-4}	3.00×10^{-4}
	Mean	2.06×10^{-4}	2.76×10^{-4}	2.03×10^{-4}	2.72×10^{-4}

Non-Carcinogenic Risk: The non-carcinogenic risk results for the metals for both children and adults are presented in Tables 8 and 9. Fe, Mn, Cr, As, and Zn had HQ values in children that ranged from 1.11×10^{-1} to 4.49×10^{-1} , 0 to 1.95×10^{-1} , 0 to 1.49×10^{-1} , 0 to 6.39×10^{-1} and 0 to 8.52×10^{-3} ; for ingestion, they ranged from 1.85×10^{-6} to 7.44×10^{-6} , 0 to 1.18×10^{-2} , 0 to 2.96×10^{-4} , 0 to 2.95×10^{-5} and 0 to 1.61×10^{-8} for inhalation and via dermal contact, they ranged from 1.78×10^{-4} to 7.19×10^{-4} , 0 to 7.78×10^{-3} , 0 to 1.19×10^{-2} , 0 to 2.49×10^{-3} and 0 to 6.82×10^{-6} respectively. The adult's HQ values for Fe, Mn, Cr, As, and Zn ranged from 1.49×10^{-1} to 6.03×10^{-1} , 0 to 3.73×10^{-1} , 0 to 2.00×10^{-1} , 0 to 8.58×10^{-1} and 0 to 1.14×10^{-2} for ingestion, they ranged from 3.94×10^{-5} to 1.59×10^{-4} , 0 to 5.87×10^{-4} , 0 to 3.18×10^{-4} , 0 to 3.17×10^{-5} and 0 to 1.73×10^{-8} for inhalation and via dermal contact, they ranged from 4.55×10^{-5} to 1.84×10^{-4} , 0 to 1.99×10^{-3} , 0 to 3.05×10^{-3} , 0 to 6.37×10^{-4} and 0 to 1.74×10^{-6} respectively.

According to Tables 8 and 9, the CDD for dermal contact is higher in children than in adults, but the CDD for

ingestion and inhalation is higher in adults. The same tables showed that CDD and HQ for both adults and children occurred in the following order: ingestion > dermal > inhalation, and that children have higher HQ values than adults in both the ingestion and inhalation pathways, while adults have higher HQ values than children in the dermal contact pathway. In addition to Yi, et al (2022), and Ren et al., (2019), several other researchers have noted similar tendency.

Carcinogenic Risk: Table 10 presents the findings pertaining to the carcinogenic risk. Since the other metals lacked slope factors, only the carcinogenic risk of As (ingestion, inhalation, and dermal contact) and Cr (ingestion and inhalation) were calculated. This is consistent with the International Agency for Research on Cancer (Doabi et al., 2018; Cao et al., 2014). The mean TCR values for As and Cr were 2.06×10^{-4} and 2.03×10^{-4} for children as well 2.76×10^{-4} and 2.72×10^{-4} for adults respectively. From the result obtained the TCR values for adults were higher than those of children. The maximum values for TCR lies between 2.20×10^{-4} to 3.86×10^{-4} for both As and Cr. These

readings were above the permitted limit of 1.00×10^{-4} f, raising the probability of long-term cancer in both adults and children. As a result of this finding, As and Cr should be given significant thought for the possibility of carcinogenic risk in the study area.

CONCLUSION

The concentration, contamination and Health Risk Assessment of metals from Daglfani flood plains were investigated. The concentrations of Al, K, Fe, Mg, Zr, and La are greater than the crustal values but the concentrations of Ca, Ti, Mn, Ce, Zn, and Cr were less than the crustal values. The result of the multivariate Statistical analysis showed that the elements in PC2 (La and Cr) and PC3 (As and Zn) were also found in Cluster 1 of the HCA and they were the same elements that showed a non-significant relationship in Correlation Analysis. The result also showed that the elements in PC1 (Al, Fe, Ca, Mg, Ce, K, Ti, and Mn) of the PCA were the same elements found in C2 (Ce and Mn), C3 (Zr, Ca, Ti, and Mg), and C4 (K, Fe and Al) of the HCA. These elements were the same elements that showed Very Significant Correlation in Correlation Analysis. The result of the non-carcinogenic Health Risk Analysis showed that the CDD for dermal contact is higher in children while the CDD for ingestion and inhalation is higher in adults. The CDD and HQ in the study area is in the order: ingestion > inhalation > dermal. The result of the study also showed that children have higher HQ values in ingestion and inhalation while adults have higher HQ values in dermal pathways. For Carcinogenic Risk, the TCR values for adults are greater than those of children. The values obtained were above the permitted value of 1×10^{-4} as such raising the probability of long term cancer risk in both adult and children.

CONFLICT OF INTEREST

The authors declare that there is no conflict of interest regarding this manuscript.

REFERENCE

- Abouian, M., Ahmad, J., Zanjani, J., & Darban, A. K. (2020). Heavy metal pollution and human health risk assessment for exposure to surface soil of mining area : a comprehensive study. *Environmental Earth Sciences*, 1–18. <https://doi.org/10.1007/s12665-020-09110-3>
- Abraham, G. M. S., & Parker, R. J. (2008). Assessment of heavy metal enrichment factors and the degree of contamination in marine sediments from Tamaki Estuary , Auckland , New Zealand. *Environ Monit Assesmet* 227–238. <https://doi.org/10.1007/s10661-007-9678-2>
- Ackah, M. (2019). Soil elemental concentrations,

geoaccumulation index, non-carcinogenic and carcinogenic risks in functional areas of an informal e-waste recycling area in Accra, Ghana. *Chemosphere*, 235, 908–917.

<https://doi.org/10.1016/j.chemosphere.2019.07.014>

Adimalla, N. (2019). Heavy metals contamination in urban surface soils of Medak province , India , and its risk assessment and spatial distribution. *Environmental Geochemistry and Health*, 1(126), 59–75. <https://doi.org/10.1007/s10653-019-00270-1>

Adimalla, N., Chen, J., & Qian, H. (2020). Spatial characteristics of heavy metal contamination and potential human health risk assessment of urban soils: A case study from an urban region of South India. *Ecotoxicology and Environmental Safety*, 194(126).

Adimalla, N., & Wang, H. (2018). Distribution, contamination, and health risk assessment of heavy metals in surface soils from northern Telangana, India. *Arabian Journal of Geosciences*, 11(21).

Alshahri, F., & El-Taher, A. (2018). Assessment of Heavy and Trace Metals in Surface Soil Nearby an Oil Refinery, Saudi Arabia, Using Geoaccumulation and Pollution Indices. *Archives of Environmental Contamination and Toxicology*, 75(3), 390–401. <https://doi.org/10.1007/s00244-018-0531-0>

Cao, S., Duan, X., Zhao, X., Ma, J., Dong, T., Huang, N., Sun, C., He, B., & Wei, F. (2014). Health risks from the exposure of children to As, Se, Pb and other heavy metals near the largest coking plant in China. *Science of the Total Environment*, 472, 1001–1009.

Chandrasekaran, A., & Ravisankar, R. (2015). Spatial distribution of physico-chemical properties and function of heavy metals in soils of Yelagiri hills , Tamilnadu by energy dispersive X-ray fluorescence spectroscopy (EDXRF). *Spectrochimica Acta Part A: Molecular and Biomolecular Spectroscopy*, 150, 586–601. <https://doi.org/10.1016/j.saa.2015.05.083>

Chandrasekaran, A., Ravisankar, R., Harikrishnan, N., Satapathy, K. K., & Prasad, M. V. R. (2015). Multivariate statistical analysis of heavy metal concentration in soils of Yelagiri Hills , Tamilnadu , India – Spectroscopical approach. *Spectrochimica Acta Part A: Molecular and Biomolecular Spectroscopy* 137, 589–600.

Chimweta, M., Nyakudya, I. W., & Jimu, L. (2017). Fertility status of cultivated floodplain soils in the Zambezi Valley , northern Zimbabwe. *Physics and Chemistry of the Earth* (2017), <https://doi.org/10.1016/j.pce.2017.12.005>

Dauda, S., Kwaku, S., Amaning, K., Deinmodei, M., & Chikogu, V. (2017). Ecohydrology & Hydrobiology Preliminary investigation of flooding problems and the occurrence of kidney disease around Hadejia-Nguru wetlands , Nigeria and the need for an ecohydrology solution. *Integrative Medicine Research*, 2016. <https://doi.org/10.1016/j.ecohyd.2017.11.005>

Doabi, S. A., Karami, M., Afyuni, M., & Yeganeh, M. (2018). Pollution and health risk assessment of heavy metals in agricultural soil, atmospheric dust and major food crops in Kermanshah province, Iran. *Ecotoxicology and Environmental Safety*, 163(July), 153–164.

Ekere, J.N, Ukoha, P. O. and Ihedioha, J.N. (2016). Ecological and human health risk assessment of heavy metal contamination in soil of a municipal solid waste dump in Uyo , Nigeria. *Environmental Geochemistry and Health*. <https://doi.org/10.1007/s10653-016-9830-4>

Gupta, N., Kumar, K., Kumar, V., Cabral-pinto, M. M. S., Alam, M., Kumar, S., & Prasad, S. (2021). Appraisal of contamination of heavy metals and health risk in agricultural soil of Jhansi city , India. *Environmental Toxicology and Pharmacology*, 88(September), 103740. <https://doi.org/10.1016/j.etap.2021.103740>

Hou, D., O'Connor, D., Nathanail, P., Tian, L., & Ma, Y. (2017). Integrated GIS and multivariate statistical analysis for regional scale assessment of heavy metal soil contamination: A critical review. *Environmental Pollution*, 231, 1188–1200. <https://doi.org/10.1016/j.envpol.2017.07.021>

Hu, J., Lin, B., Yuan, M., Lao, Z., Wu, K., Zeng, Y., Liang, Z., Li, H., Li, Y., Zhu, D., Liu, J., & Fan, H. (2019). Trace metal pollution and ecological risk assessment in agricultural soil in Dexing Pb/Zn mining area, China. *Environmental Geochemistry and Health*, 41(2), 967–980. <https://doi.org/10.1007/s10653-018-0193-x>

Hussain, R., Luo, K., Chao, Z., & Xiaofeng, Z. (2018). Trace elements concentration and distributions in coal and coal mining wastes and their environmental and health impacts in Shaanxi , China. *Environmental Science and Pollution Research*, 25(20): 19566-19584,

Ilechukwu, I., Osuji, L. C., Peter, C., Onyema, M. O., & Ndukwe, G. I. (2021). Assessment of heavy metal pollution in soils and health risk consequences of human exposure within the vicinity of hot mix asphalt plants in Rivers State , Nigeria. *Environmental Monitoring and Assessment*. <https://doi.org/10.1007/s10661-021-09208-6>

Jiang, F., Ren, B., Hursthouse, A., Deng, R., & Wang, Z. (2019). Distribution, source identification, and ecological-health risks of potentially toxic elements (PTEs) in soil of thallium mine area (southwestern Guizhou, China). *Environmental Science and Pollution Research*, 26(16), 16556–16567. <https://doi.org/10.1007/s11356-019-04997-3>

Jiang, Y., Chao, S., Liu, J., Yang, Y., & Chen, Y. (2017). Source apportionment and health risk assessment of heavy metals in soil for a township in Jiangsu Province , China. *Chemosphere*, 168, 1658–1668. <https://doi.org/10.1016/j.chemosphere.2016.11.088>

Jin, Y., O'Connor, D., Ok, Y. S., Tsang, D. C. W., Liu, A., & Hou, D. (2019). Assessment of sources of heavy metals in soil and dust at children's playgrounds in Beijing using GIS and multivariate statistical analysis. *Environment International*, 124(November 2018), 320–328. <https://doi.org/10.1016/j.envint.2019.01.024>

Kabata, P. A. and Pendias, H (2010), Trace Elements in Soil and Plants, *CRC Press*, Boca Raton, FL, USA, 2000. (pp. 67–83).

Krishna, A. K., & Mohan, K. R. (2016). Distribution , correlation , ecological and health risk assessment of heavy metal contamination in surface soils around an industrial area , Hyderabad , India. *Environmental Earth Sciences*. <https://doi.org/10.1007/s12665-015-5151-7>

Ma, L., Sun, J., Yang, Z., & Wang, L. (2015). Heavy metal contamination of agricultural soils affected by mining activities around the Ganxi River in Chenzhou, Southern China. *Environmental Monitoring and Assessment*, 187(12), 1–9. <https://doi.org/10.1007/s10661-015-4966-8>

Mamat, Z., Haximu, S., Zhang, Z., & Aji, R. (2018). An ecological risk assessment of heavy metal contamination in the surface sediments of Bosten Lake , northwest China. 23(April 2016).

Mohammadi, A. A., Zarei, A., Esmaeilzadeh, M., Taghavi, M., Yousefi, M., Yousefi, Z., Sedighi, F., & Javan, S. (2019). Assessment of Heavy Metal Pollution and Human Health Risks Assessment in Soils Around an Industrial Zone in Neyshabur , Iran. *Biological Trace Element Research* <https://doi.org/10.1007/s12011-019-01816-1>

Aluko, T.S., Njoku, K.L., Adesuyi, A.A., Akinola, M.O. (2018). Health Risk Assessment of Heavy Metals in Soil from the Iron Mines of Itakpe and Agbaja , Kogi State , Nigeria. *Pollution*, 4(3): 527-538. <https://doi.org/10.22059/poll.2018.243543.330>

- Narsimha A., Jie C., and Hui, Q (2020). Spatial characteristics of heavy metal contamination and potential human health risk assessment of urban soils : A case study from an urban region of South India. *Ecotoxicology and Environmental Safety* 194 (2020) 110406Tirumalgiy
- Ngwese, S. N., Mouri, H., Akoachere, R. A. I. I., McKinley, J. M., & Candeias, C. (2025). Sources, Pathways, and Health Risk Assessment of Harmful Elements in Soil and Crops: A Case Study from East Cameroon. *Exposure and Health*, 0123456789. <https://doi.org/10.1007/s12403-025-00714-3>
- Ni, M., Mao, R., Jia, Z., Dong, R., & Li, S. (2018). Heavy metals in soils of Hechuan County in the upper Yangtze (SW China): Comparative pollution assessment using multiple indices with high-spatial-resolution sampling. *Ecotoxicology and Environmental Safety*, 148(July 2017), 644–651. <https://doi.org/10.1016/j.ecoenv.2020.117>
- Obiri-nyarko, F., Duah, A. A., Karikari, A. Y., Agyekum, W. A., Manu, E., & Tagoe, R. (2021). Assessment of heavy metal contamination in soils at the Kpone landfill site , Ghana : Implication for ecological and health risk assessment. *Chemosphere*, 282(December 2020), 131007.
- Ogunleye, A.O. and Akinrinde, S. A. (2025). Assessment of Heavy Metals and Physicochemical Properties from Artisanal Mining Site at Rimin Zayam Toro Local Government Area of Bauchi State,Nigeria *Journal of Basics and Applied Sciences Research* ,3(3),168-176. <https://dx.doi.org/10.4314/jobasr.v3i3.18168>
- Orisakwe, K. U. (2013). Change Detection Analysis of Landuses in Hadejia township of Jigawa State of Nigeria. *International Journal of Applied Science and Technology* 3(3), 160–168.
- Oyedotun, T. D. T. (2018). X-ray fluorescence (XRF) in the investigation of the composition of earth materials: a review and an overview. *Geology, Ecology, and Landscapes*, 2(2), 148–154. <https://doi.org/10.1080/24749508.2018.1452459>
- Pablo, P., Toro, V., Fernando, L., Bedoya, V., Darío, I., Rocío, G., Franco, B., Alcántara-carrió, J., Alberto, J., & Baena, P. (2016). Impact of terrestrial mining and intensive agriculture in pollution of estuarine surface sediments : Spatial distribution of trace metals in the Gulf of Urabá , Colombia. *MPB*. <https://doi.org/10.1016/j.marpolbul.2016.06.093>
- Penteado, J. O., Brum, R. de L., Ramires, P. F., Garcia, E. M., dos Santos, M., & da Silva Júnior, F. M. R. (2021). Health risk assessment in urban parks soils contaminated by metals, Rio Grande city (Brazil) case study. *Ecotoxicology and Environmental Safety*, 208. <https://doi.org/10.1016/j.ecoenv.2020.117>
- Pobi, K. K., Nayek, S., Gope, M., Rai, A. K., & Saha, R. (2020). Sources evaluation, ecological and health risk assessment of potential toxic metals (PTMs) in surface soils of an industrial area, India. *Environmental Geochemistry and Health*, 42(12), 4159–4180. <https://doi.org/10.1007/s10653-020-0>
- Pujiwati, A., Nakamura, K., Watanabe, N., & Komai, T. (2018). Application of multivariate analysis to investigate the trace element contamination in top soil of coal mining district in Jorong, South Kalimantan, Indonesia. *IOP Conference Series: Earth and Environmental Science*, 118(1). <https://doi.org/10.1088/1755-1315/118/1/012062>
- Qishlaqi, A., & Moore, F. (2007). Statistical Analysis of Accumulation and Sources of Heavy Metals Occurrence in Agricultural Soils of Khoshk River Banks , Shiraz , Iran. *American-Eurasian J. Agric. & Environ. Sci.*, 2(5), 565–573.
- Ren, Z., Xiao, R., Zhang, Z., Lv, X., & Fei, X. (2019). Risk assessment and source identification of heavy metals in agricultural soil : a case study in the coastal city of Zhejiang. *Stochastic Environmental Research and Risk Assessment*, 8. <https://doi.org/10.1007/s00477-019-01741-8>
- Shackley, M. S. (2018). X-Ray Fluorescence Spectrometry (XRF). *The Encyclopedia of Archaeological Sciences*, 1–5. <https://doi.org/10.1002/9781119188230.saseas0620>
- Soltani-gerdefaramarzi, S., Ghasemi, M., & Ghanbarian, B. (2021). Geogenic and anthropogenic sources identification and ecological risk assessment of heavy metals in the urban soil of Yazd , central Iran. *PLoS ONE* 16(11), 1–14. <https://doi.org/10.1371/journal.pone.0260418>
- Thongyuan, S., Khantamoon, T., Aendo, P., Binot, A., & Tulayakul, P. (2021). Ecological and health risk assessment, carcinogenic and non-carcinogenic effects of heavy metals contamination in the soil from municipal solid waste landfill in Central, Thailand. *Human and Ecological Risk Assessment*, 27(4), 876–897. <https://doi.org/10.1080/10807039.2020.1786666>

- Turekian, K. K., & Wedephol, K. H. (1961). Distribution of the elements in some major units of the earth's crust. *Geological Society of America Bulletin*, 72, 175–192
- Wang, F., Guan, Q., Tian, J., Lin, J., Yang, Y., Yang, L., & Pan, N. (2020). Contamination characteristics, source apportionment, and health risk assessment of heavy metals in agricultural soil in the Hexi Corridor. *Catena*, 191(April 2019), 104573. <https://doi.org/10.1016/j.catena.2020.104573>
- Wu, J., Lu, J., Li, L., Min, X., & Luo, Y. (2018). Chemosphere Pollution, ecological-health risks, and sources of heavy metals in soil of the northeastern Qinghai-Tibet Plateau. *Chemosphere*, 201, 234–242. <https://doi.org/10.1016/j.chemosphere.2018.02.122>
- Wu, W., Wu, P., Yang, F., Sun, D., Zhang, D., & Zhou, Y. (2018). Environment Assessment of heavy metal pollution and human health risks in urban soils around an electronics manufacturing facility. *Science of the Total Environment*, 630, 53–61. <https://doi.org/10.1016/j.scitotenv.2018.02.183>
- Yang, S., Zhao, J., Chang, S. X., Collins, C., Xu, J., & Liu, X. (2019). Status assessment and probabilistic health risk modeling of metals accumulation in agriculture soils across China: A synthesis. *Environment International*, 128(March), 165–174. <https://doi.org/10.1016/j.envint.2019.04.044>
- Yaw, G., Godwin, H., David, A. A., & Shiloh, K. E. (2019). Contamination impact and human health risk assessment of heavy metals in surface soils from selected major mining areas in Ghana. *Environmental Geochemistry and Health*, 4. <https://doi.org/10.1007/s10653-019-00332-4>
- Yi, Y. & H. L. (2022). Spatial distribution and source identification for heavy metals in surface sediments of East. *Scientific Reports*, 12, 1–9. <https://doi.org/10.1038/s41598-022-12148-x>
- Zhang, P., Qin, C., Hong, X., Kang, G., Qin, M., Yang, D., Pang, B., Li, Y., He, J., & Dick, R. P. (2018). Risk assessment and source analysis of soil heavy metal pollution from lower reaches of Yellow River irrigation in China. *Science of the Total Environment*, 633, 1136–1147. <https://doi.org/10.1016/j.scitotenv.2018.03.228>
- Zheng, X., Chen, M., Wang, J., Li, F., & Liu, Y. (2020). Soil and Sediment Contamination: An International Ecological Risk Assessment of Heavy Metals in the Vicinity of Tungsten Mining Areas, Southern Jiangxi Province Ecological Risk Assessment of Heavy Metals in the Vicinity of. *Soil and Sediment Contamination: An International Journal*, 00(00), 1–15. <https://doi.org/10.1080/15320383.2020.1763912>
- Zhushan, F., & Shuhua, X. (2019). The Effects of Heavy Metals on Human Metabolism. *Toxicology Mechanisms and Methods*, 0(0), 000. <https://doi.org/10.1080/15376516.2019.1701594>